

Investigation of Defect Generation and Propagation in Electrically and Photonically Stressed Silicon Carbide

Hongyu Peng^{1,a*}, Yafei Liu^{1,b}, Zeyu Chen^{1,c}, Qianyu Cheng^{1,d},
Shanshan Hu^{1,e}, James Watson^{2,f}, Kristin Sampayan^{2,g},
Stephen Sampayan^{2,3,h}, Balaji Raghothamachar^{1,i} and Michael Dudley^{1,j}

¹Materials Science and Chemical Engineering, Stony Brook University, Stony Brook, New York, 11794, USA

²Opcondys Incorporated, 600 Commerce Court, Manteca, CA, 95336, USA

³Lawrence Livermore National Laboratory, 7000 East Avenue, Livermore, CA, 94551, USA

^ahongyu.peng@stonybrook.edu, ^byafei.liu@stonybrook.edu, ^czeyu.chen@stonybrook.edu,

^dqianyu.cheng@stonybrook.edu, ^eshanshan.hu@stonybrook.edu, ^fmudman1960@gmail.com,

^gkristinsa@opcondys.com, ^hstephensa@opcondys.com, ⁱbalaji.raghothamachar@stonybrook.edu,

^jmichael.dudley@stonybrook.edu

Keywords: Synchrotron X-ray topography, dislocations, photoconductive semiconductor switches

Abstract. A highly efficient, high-voltage power switching technology, the Optical Transconductance Varistor (OTV) is being developed based on the photoconductive property of 6H-SiC. The behavior of the dislocations in 6H-SiC under the application of voltage and laser in such devices is of particular interest. In this study, both ex-situ and in-situ synchrotron X-ray topography were applied to characterize dislocations and investigate their behaviors when the sample was electrically and photonically stressed. Threading dislocations (TDs) and basal plane dislocations (BPDs) were revealed in transmission topographs and grazing topographs. When the samples were connected to external voltage ranging from 1kV to 4kV, there were no observable signs of dislocation movement. This indicates that the energy released from the transitioning of Vanadium states is lower than the activation energy for dislocation gliding.

Introduction

Si and GaAs based photoconductive semiconductor switches (PCSS) have been investigated since the 1980's [1]. With the development of crystal growth techniques, high quality wide bandgap semiconductor materials have become commercially available, and 6H-SiC is being applied in PCSS due to its semi-insulating properties. This material is normally insulating but when illuminated, either the charge carriers from the valence band jump to the conduction band or the excitation of deep states makes it conductive in proportion to the light intensity [2]. A highly efficient, high-voltage power switching technology, the Optical Transconductance Varistor (OTV) is being developed based on the photoconductive property of 6H-SiC [3,4,5]. OTV differs from other PCSS in that it provides bidirectional linear control over voltage and current where other devices only provide on-off control.

SiC crystals are usually characterized by significant densities of defects including threading dislocations (TDs), basal plane dislocations (BPDs) and occasionally stacking faults that are generated when the crystal is grown usually by the PVT method. Under the application of high voltage and laser in the OTV, the configuration of defects can potentially change and that might adversely impact the performance of the device. The behavior of defects in material subjected to electrical stress has been well documented [7-9], but their response to the simultaneous application of high electric field and intense light has not been studied. The recombination process can release energy in the form of phonons into the crystal lattice which may generate, propagate and/or convert defects. These defects may eventually limit the carrier lifetime in the device. Therefore, characterization and understanding the mechanism of potentially destructive defects is of great scientific interest as well to the development of the OTV device.

Synchrotron X-ray topography (XRT) is a powerful and non-destructive technique that enables imaging large area crystals with high resolution, where extended defects such as dislocations, stacking faults and grain boundaries in crystals can be revealed [10]. In this study, XRT is applied to characterize the dislocations and the configurations are determined. The movement of dislocations was also investigated by analyzing the topographic images that were recorded when the sample was photonically and electrically stressed. Preliminary results indicate that threading screw/mixed dislocations (TSD/TMD) are unaffected when the wafer was stressed. Most of the BPDs and threading edge dislocations (TEDs) also do not show observable signs of movement.

Experiments

In this study, the samples being used for PCSS development are (11 $\bar{2}$ 0) 6H-SiC semi-insulating axial wafers (on-axis). The thickness of the sample is approximately 386 μm and the surface is finished by chemical mechanical polishing. Two sets of experiments were carried out, 1) Recorded X-ray topographs of the samples without external conditions (ex-situ experiments). 2) Recorded X-ray topographs of the samples when it was electrically and photonically stressed (in-situ experiments). Ex-situ experiment set up is shown in Fig. 1, where the commonly used geometries were applied, i.e., grazing incidence geometry (Fig. 1 (a)) and transmission geometry (Fig. 1 (b)).

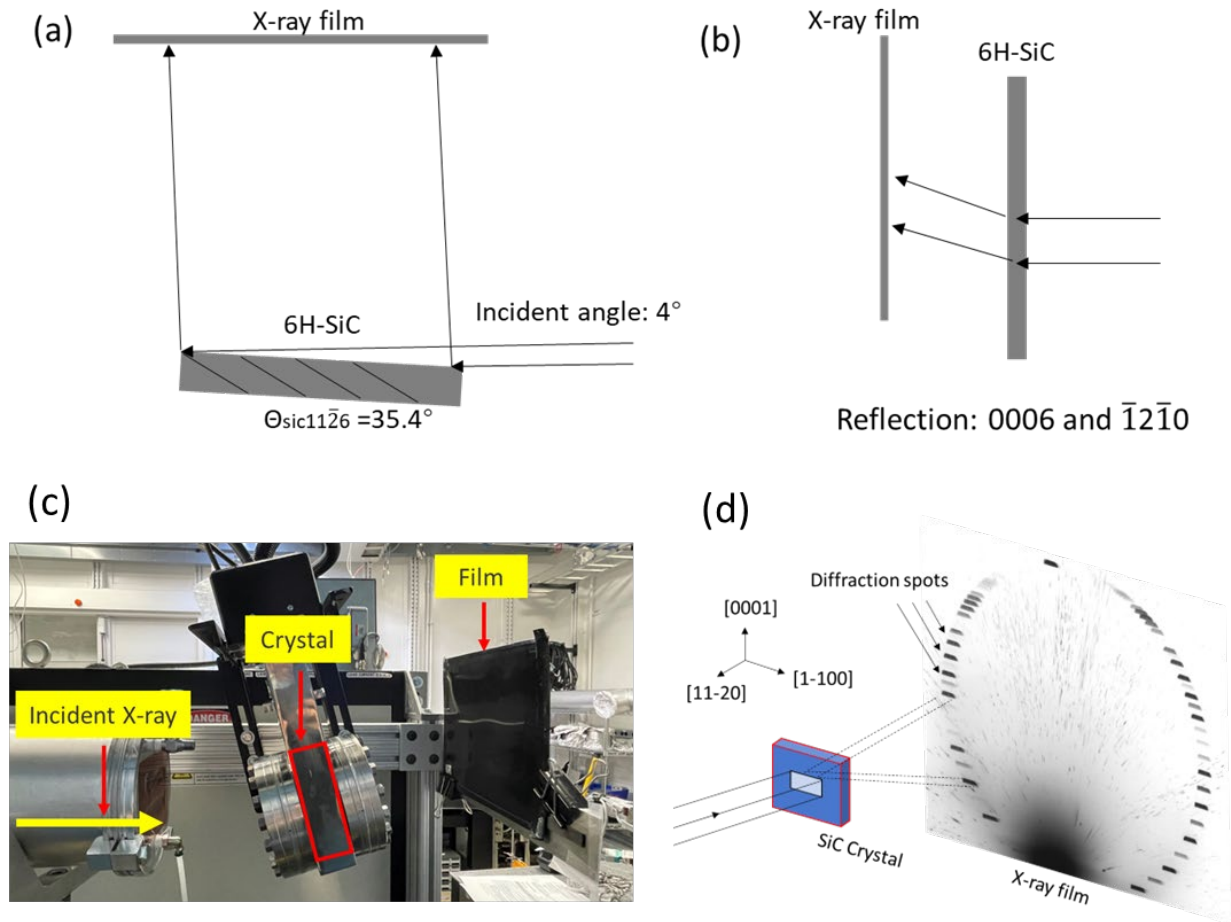


Figure 1. The geometries of the experimental set ups for (a) grazing incidence topography and (b) transmission topography. (c) In-situ experimental set up (SiC crystal mounted in the chamber, X-ray film was used to record images). (d) X-ray diffraction pattern of the sample.

But during in-situ experiments, the sample was placed in a holder that was illuminated and connected to external voltage. Therefore, sample and detector placement flexibilities were limited. Although synchrotron X-ray grazing incidence topography showed clear defect contrast, it is not applicable for in-situ experiments because of the limitations of the apparatus. Therefore, synchrotron

white beam X-ray topography in transmission geometry was used to image the samples at a limited range of incident angles (Fig. 1 (c)). The experiments were carried out at 1-BM station, Advanced Photon Source in Argonne National Laboratory.

As white beam has X-ray energy over a wide range, diffraction spots from different lattice planes can be detected (Fig. 1 (d)). X-ray films were placed $\sim 200\text{mm}$ away from the sample to record the diffraction spots (Fig. 1 (c)). Since the structure factors of different lattice planes vary, the diffraction intensity and the contrast of each spot can be different. Some of the diffraction spots with clear contrast were selected and the behaviors of the defects under the condition of illumination and high voltage were analyzed (the chamber was rotated by $\sim 15^\circ$ (Fig. 1 (c)) to get higher diffraction intensity and corresponding better image contrast). Details of the conditions applied to the samples are shown in Table 1. Sample A was characterized by regular X-ray topography without any applied conditions. 1 kV voltage was applied to sample B for 300 minutes while sample C was connected to a voltage at 1.9 kV. Sample D was first connected to 2 kV for 120 minutes and then the voltage was increased to 2.5 kV and 4 kV for 180 minutes and 60 minutes respectively. For photonic stressing, pulsed laser at 1.3 eV was applied for sample B, C and D.

Table 1. Experiment details of the samples

Sample	Experimental Steps
A	Untreated
B	1.0 [kV], 300 [min]
C	1.9 [kV], 300 [min]
D	2 [kV], 120 [min] 2.5 [kV], 180 [min] 4 [kV], 60 [min]

Results and Discussion

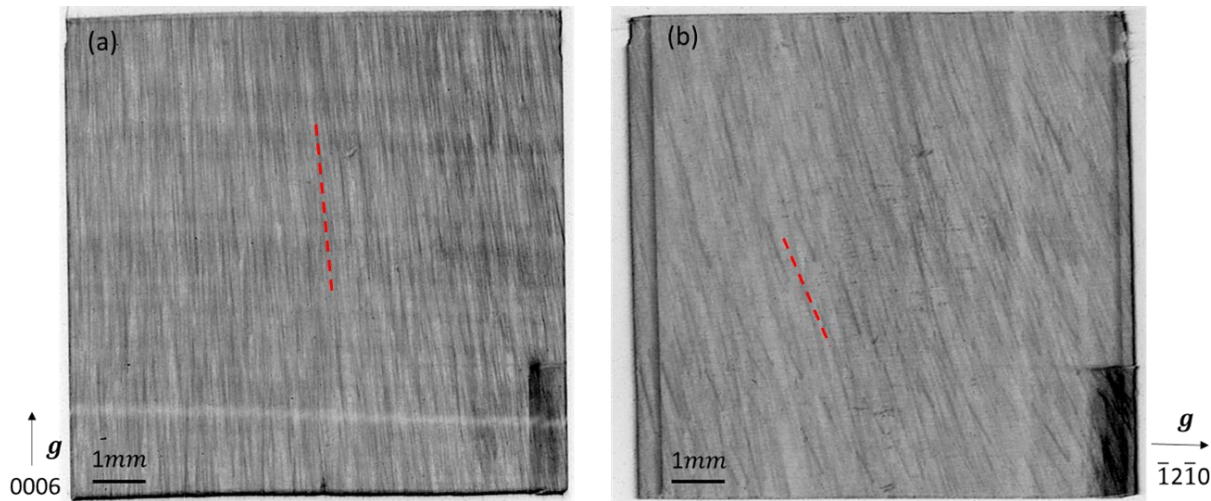


Figure 2. Synchrotron X-ray transmission topographs of threading dislocations in sample A in (a) 0006 reflection, (b) $\bar{1}2\bar{1}0$ reflection. The vertical linear features in 0006 reflection are TSDs while the linear features in the $\bar{1}2\bar{1}0$ reflection are TEDs. The line directions of the TSDs/TEDs is indicated by the dashed red line. From the topographs, it is clear that TSDs are almost along c-axis (the vertical direction) while TEDs can be several degrees off c-axis.

Overall transmission topograph of sample A is shown in Fig. 2. Investigation of TDs was carried out. Fig. 2 shows the 0006 and $\bar{1}2\bar{1}0$ transmission topographs of a 6H-SiC sample. The line directions of threading dislocations are almost along the vertical direction (c-axis), but they could still be off c-axis during growth. According to $\mathbf{g} \cdot \mathbf{b} = 0$ and $\mathbf{g} \cdot \mathbf{b} \times \mathbf{l} = 0$ criteria, the TEDs ($\mathbf{b} = 1/3(11\bar{2}0)$) will be out of contrast in Fig. 2 (a) since the reflection vector is 0006. Similarly, the

TSDs ($\mathbf{b} = [0001]$) will not significantly contribute to the contrast in Fig. 2 (b). Therefore, the dislocations showing contrast in Fig. 2 (a) are most likely TSDs while the dislocations in Fig. 2 (b) are TEDs. Comparing the dislocations in Fig. 2 (b) to that in Fig. 2 (a), it is obvious that TEDs have larger inclination angle to c-axis (vertical lines appear tilted top left to bottom right) while TSDs are almost parallel to c-axis. As the Burgers vector of TSDs is around 6 times that of TEDs, it will be energetically unfavorable for those dislocations to deviate from the c-axis because of larger line tension. The magnified grazing incidence topograph of the sample is shown in Fig. 3, where the white feature along with black contrast on the right is TD (they are almost along c-axis). BPDs, however, show contrast either as short horizontal segments or white dots, depending on their relative line directions with respect to the sample surface ($11\bar{2}0$).

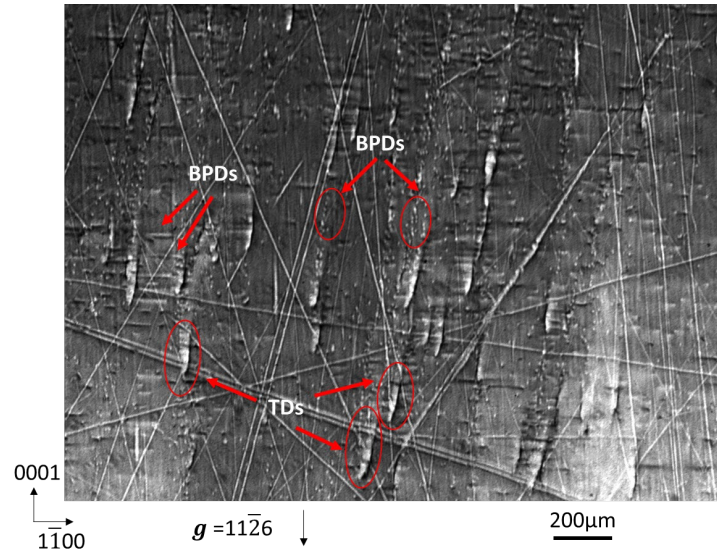


Figure 3. Grazing incidence topographic image of the sample that was not subjected to external conditions. TDs and BPDs are marked. The straight lines crossing the topograph are scratches.

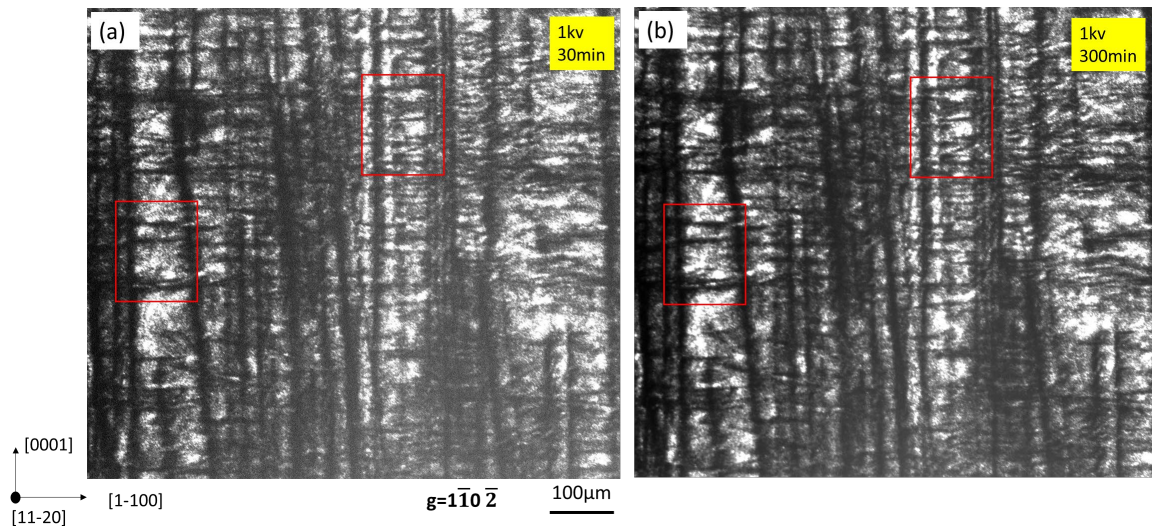


Figure 4. Topographic image of sample B that was photonically and electrically stressed for 30 minutes (a) and 300 minutes (b). The dark linear features along vertical direction are threading dislocations, while the dark segments along horizontal direction as marked by the red boxes are BPDs.

Though basic dislocation information was revealed in ex-situ experiments, potential migration of the dislocations under external condition still requires further investigation. Therefore, sample B was mounted in a chamber that was connected to external voltage at 1 kV and the sample was illuminated by laser through a fiber. Then the sample was photonically and electrically stressed for 5 hours. Topographic images were recorded every 10 minutes and two selected images are shown (i.e. after

being stressed for 30 minutes and 300 minutes) in Fig. 4. The vertical linear black features are TDs and the horizontal black segments are BPDs. Because the sample was rotated by 15° , basal planes are no longer parallel to the film. The projection of basal plane leaves a small height (thickness of the sample times $\tan 15^\circ = 78\mu\text{m}$) on the X-ray films, indicating that the behavior of BPDs can be recorded. However, from these topographs with best contrast, no dislocation migrations are observed. Some of the BPDs are marked by the red boxes for illustration purpose (Fig. 4).

As the voltage applied to sample B is relatively low (1 kV), higher voltages were employed for samples C and D. The magnified topographic images of sample C are shown in Fig. 5. As c-axis is along horizontal direction in Fig. 5, BPDs are visible as vertical segments while TDs are along the horizontal direction all the way through the topograph. The red box shows a minor sign of change in contrast, which most likely comes from slight change to the sample mounting condition over time and is not microstructure-related. No changes in defect configuration has been observed.

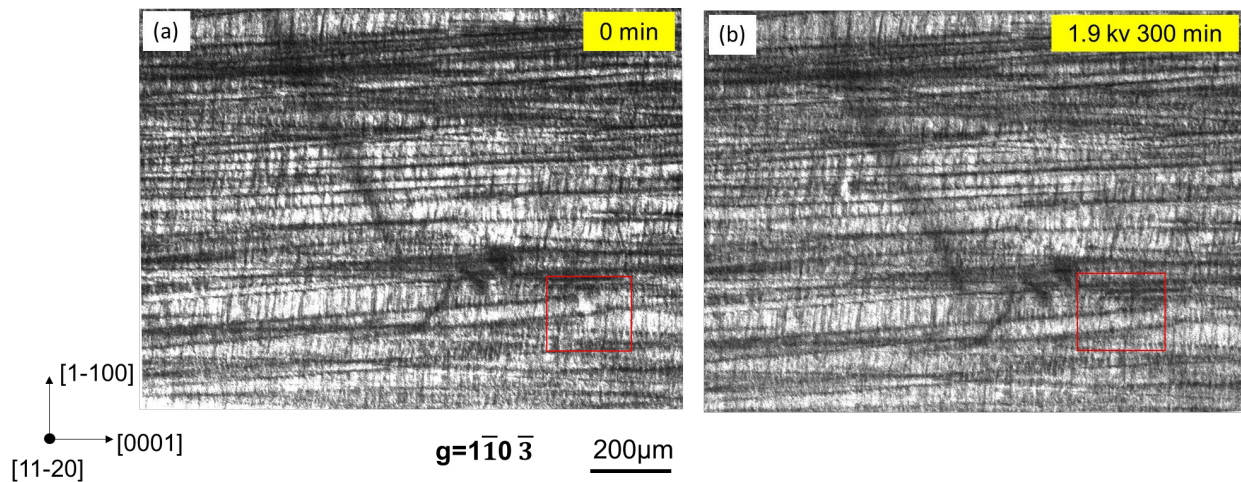


Figure 5. Comparison between the topographic image of sample C (a) before applying stress, and (b) after photonically and electrically stressed for 300 minutes under 1.9 kV.

Similar to sample C, there is a red box that shows a minor sign of change in contrast in sample D. This is not considered as microstructure-related feature. No changes in defect configuration have been observed even though the voltage was increased to 4 kV (Fig. 6).

By comparing these topographic images, we can conclude that threading dislocations (the linear features almost vertically (sample A and B) or horizontally (sample C and D) across the image) are unaffected. This observation is expected since TSDs/TMDs are sessile (immobile) and TEDs can only glide on secondary prismatic slip planes. More importantly, BPDs do not show any observable signs of migration as well. This could be explained as follows:

When OTV is working, electrons are excited from deep Vanadium state [5]. The energetics of transitioning of the state (neutral/acceptor/donor state of Vanadium) is low enough that the migration of BPDs or the formation of killer defects did not occur. According to a previous study [11], the activation energy for dislocation gliding in SiC is 2.5 eV. This value could be fairly large compared to the energies released from the transitioning of the state. Additionally, in our experiments, the recombination enhanced dislocation glide process does not appear to have occurred, though this process could reduce the activation energy from 2.5 eV to 0.2~0.3 eV. The energy of laser used (1.3 eV) is also too low for dislocation glide to be activated.

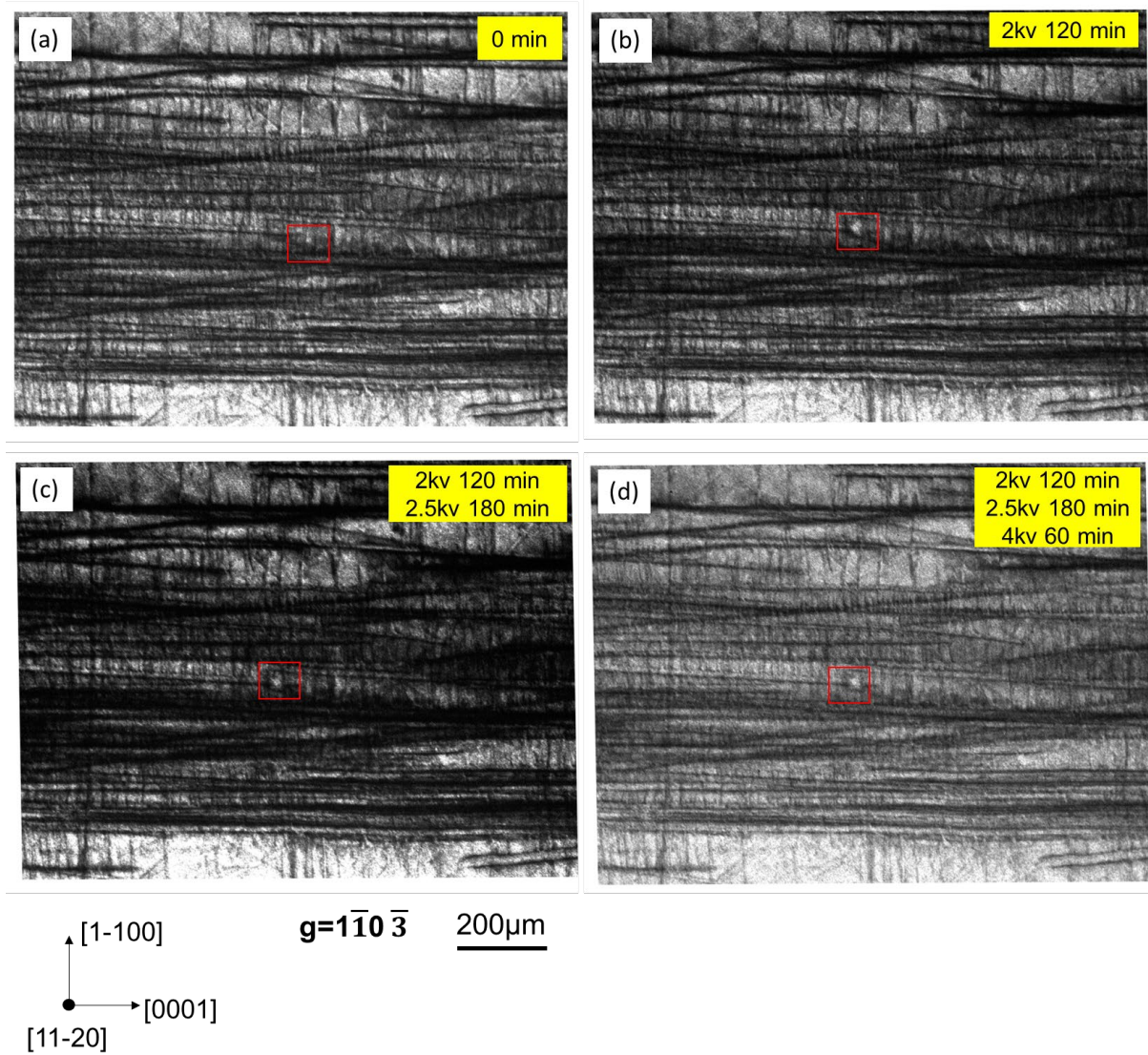


Figure 6. Topographic images of sample D that was at different experimental stages indicated by the information inside the yellow boxes.

Summary

Ex-situ and in-situ experiments were carried out at Advanced Photon Source in Argonne National Laboratory (Table 1) to study the impact of electrically and photonically stressing on dislocation microstructure in 6H-SiC semi-insulating wafers. Ex-situ topographic image revealed the BPDs and TDs in the sample. While the results of in-situ experiments indicate that there are only minor changes in contrast in the topographs, but dislocations do not move. This could be explained as the activation energy of BPD gliding is relatively high while the energies released from the transitioning of Vanadium state is too low.

Acknowledgement

The information, data, or work presented herein was funded in part by the Advanced Research Projects Agency-Energy (ARPA-E), U.S. Department of Energy, under Award Number DE-AR0000907. This research used resources of the Advanced Photon Source (Beamline 1-BM). The Joint Photon Sciences Institute at Stony Brook University provided partial support for travel and subsistence at the Advanced Photon Source.

References

- [1] W.C. Nunnally and R. B. Hammond, Appl. Phys. Lett. 44, 980-982 (1984).
- [2] S.E. Sampayan, M. Bora, C. Brooksby, G.J. Caporaso, A. Conway, S. Hawkins, B. Hickman, C. Holmes, H. Nguyen, R. Nikolic, D. Palmer, L. Voss, L. Wang, & A. Waters. Mater. Sci. Forum, 821–823, 871 (2015).
- [3] P.S. Cho, J. Goldhar, C.H. Lee, S.E. Sadow & P. Neudeck, J. Appl. Phys., 77, 1591-1599 (1995)
- [4] S. Dogan, A. Teke, D. Huang, H. Morkoc, C. B. Roberts, J. Parish, B. Ganguly, M. Smith, R. E. Myers & S. E. Sadow, Appl. Phys. Lett., 82, 3107, (2003)
- [5] S.E. Sampayan, P.V. Grivickas, A.M. Conway, K.C. Sampayan, I. Booker, M. Bora, G.J. Caporaso, V. Grivickas, H.T. Nguyen, K. Redekas, A. Schoner, L. F. Voss, M. Vengris & L. Wang, Sci. Rep. 11, 6859 (2021)
- [6] P.J. Wellmann, Semiconductor Science and Technology 33, 103001 (2018).
- [7] P.G. Neudeck, J.A. Powell, IEEE Electron. Dev. Lett., 15, 63 (1994).
- [8] P. Neudeck, W. Huang, and M. Dudley, IEEE Trans. Electron. Dev., 46, 478 (1999).
- [9] H. Chen, B. Raghathamachar, W. Vetter, M. Dudley, Y. Wang, B.J. Skromme, Mater. Res. Soc. Symp. Proc., 911, 169 (2006).
- [10] Raghathamachar B. & Dudley M. X-Ray Topography, in ASM Handbook, pp. 459-477, ASM International, DOI: <https://doi.org/10.31399/asm.hb.v10.a0006644> (2019).
- [11] A. Galeckas J. Linnros and P. Pirouz, Appl. Phys. Lett. 81, 883 (2002).